

Analysis of a Novel Proton Absorber Geometry for the Mu2e Experiment

Daniel Pershey^{a,b}, John Alsterda^a, Grace Bluhm^{a,c}, George Gollin^{a,†}, Tim He^a, Guangyong Koh^a,
Matthew McHugh^a

^aDepartment of Physics, University of Illinois at Urbana-Champaign

^bDepartment of Physics, Harvard University

^cDepartment of Physics, University of Wisconsin-Whitewater

August 7, 2009

Abstract

This paper analyzes the effects of inserting both a cylindrical and a helical proton absorber into the Mu2e detector. The paper includes a technical description of both absorbers. Monte Carlo simulations were developed to compare these two geometries. The paper describes these simulations and their results. The paper presents data from the simulations which describe the relative efficiencies of both absorbers for eliminating background protons produced in the target and information on the resolutions obtained with each absorber. The paper also analyzes the effects the absorber has on electrons injected into the downstream end of the Mu2e detector for a proposed in situ calibration.

I. Background and Introduction

The proposed Mu2e experiment at Fermilab hopes to detect events of muon conversions from the $\mu \rightarrow e$ channel in the presence of a parent nucleus. The collaboration hopes the apparatus will be able to detect about 5 such events in 10^{16} muon decays¹ which would reduce the experimental limit on the branching ratio for this channel by four orders of magnitude.

This process is forbidden in the standard model, so detection of such an event would open the scientific community to a world of interesting physics we have yet to understand. It would also help define parameters of theories beyond the standard model to guide future experiments into probing the right energies for relevant new physics.

In the experiment, a series of aluminum targets are bombarded with a low momentum muon beam. Some muons are captured by an aluminum nucleus and decay. Most decays will happen through the preferred mode

$$\mu \rightarrow \nu_{\mu} \bar{\nu}_e e$$

with a typical electron momentum of about half the muon mass. But, by energy conservation, the

electron produced in the process $\mu \rightarrow e$ will have an energy very near the muon energy. So, the signal for this experiment is an outgoing electron with an energy very near the muon mass.

Unfortunately, in the experiment there will be many muons colliding with the aluminum targets which will create a barrage of unwanted particles coming from the target overwhelming the detector with background. So, in order to distinguish a small signal from the background there must be some way to reduce the large number of particles coming from the target. One common background is a proton ejected from a parent aluminum nucleus.

II. Description of Absorber

A conventional design for the proton absorber is a 2.5 m long, .5 mm thick cylinder made from polyethylene. The problem with this proton absorber is that signal electrons pass through just as much material on average as the proton background which will decrease the sensitivity of the detector. This paper compares this conventional absorber with a novel geometry. This new absorber geometry is based on two

[†] Contact person: George Gollin, g-gollin@illinois.edu, +1 (217) 333-4451

asymmetries to preferentially stop protons while leaving electrons untouched; images are shown in Figure 1.

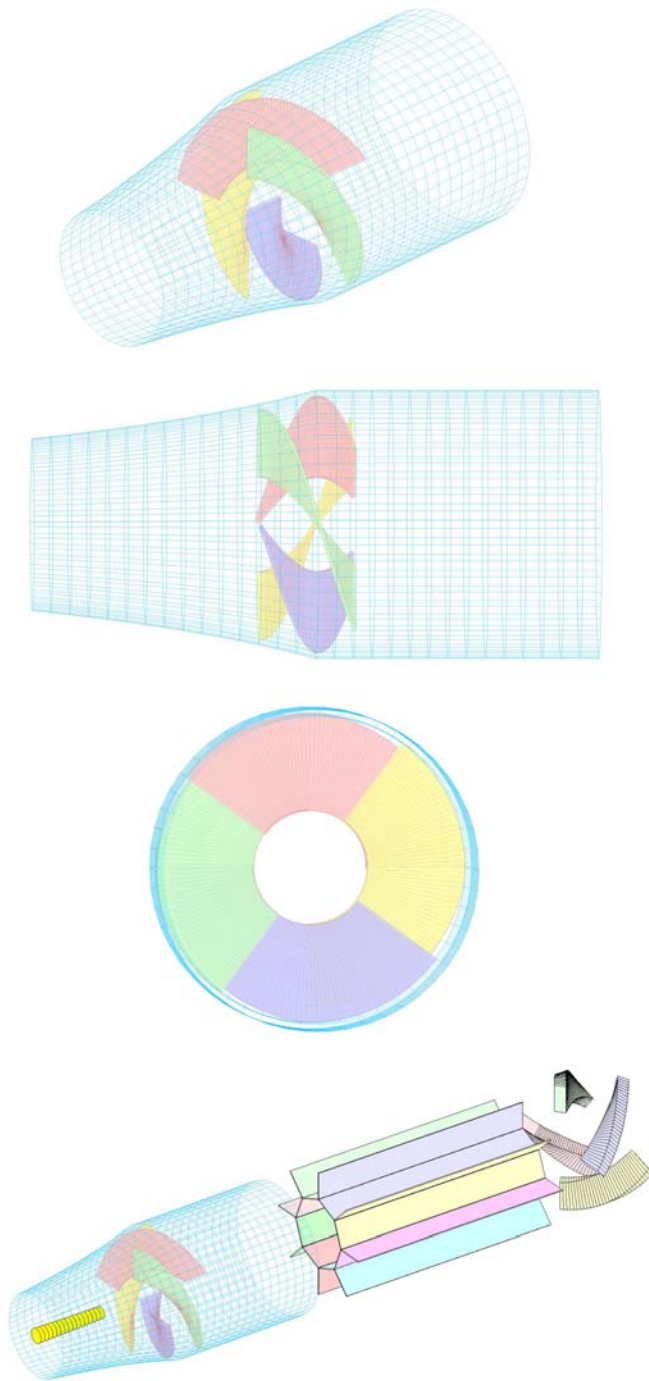


Figure 1. Four views of the absorber. Absorber viewed from an off angle (top), perpendicular to the beam (top middle), from the beam looking upstream (bottom middle), and the absorber with the detector (bottom).

Calculations² show that protons originating in

the target will have momenta between 140 and 300 MeV/c which is significantly more than the momentum of signal electrons. The experiment has a magnetic field in the detector which is roughly 1T in the beam direction around the absorber. From the cyclotron radius formula and the particle momenta, protons will travel further from the beam than electrons. So, this new absorber features a polyethylene shell around the beam. The shell starts at the first aluminum target and ends 2 m downstream of the first target. The thickness is 3 cm and the radius of the shell is given by

$$r(z) = .52 + z / 6 \quad 0 < z < 1.5$$

$$r(z) = .72 \quad 1.5 \leq z < 2$$

where r is the shell radius in meters and z is the distance downstream of the target in meters.

Since protons and electrons have opposite charges, they will follow helical trajectories spinning in opposite directions. The interior of the absorber is shaped like 4 helical arcs (“tines”) to exploit this difference in orbit helicity. Each tine is designed so that if an average electron started at the upstream end of a tine, its subsequent trajectory would lie entirely on the surface of the tine. This way, there will be many electrons that pass through the absorber region without entering the absorber material. On the other hand, protons will hit the tines at an angle $\sim 90^\circ$ and will travel through a tine on average twice as often as they would if the tines were planar. Therefore, this helical shape will stop protons twice as fast, but electrons will tend to pass through the vacuum between the tines.

In the plane perpendicular to the beam, each tine is a rectangle that starts 25 cm from the beam and continues to the inside of the shell and is 8 mm thick. The tines extend 50 cm in the direction parallel to the beam. They start 40 cm after the last aluminum target and spiral 5 radians per meter of distance parallel to the beam.

III. Method

Using Matlab, simulation programs were developed to model particle tracks in the Mu2e detector that originated in the stopping target. The 17 aluminum foil stopping targets are modeled as a uniform cylinder of radius 7 cm and

length 85 cm for a reasonable approximation.

To describe the initial position of a particle, the programs generate a random point in the modeled target assuming that each volume element had an equal probability of ejecting a particle. Similarly, the programs generate an initial momentum with each direction equally likely. Due to geometric acceptance, however, only those electrons with an angle between the momentum vector and forward axis of 60-120° were generated. For electrons, the magnitude of the momentum is assumed to be 105 MeV/c to mimic behavior of signal electrons traveling through the detector. For protons coming out of the target, a non-uniform distribution of proton energies is used. Proton kinetic energies range from 10-50 MeV with probability

$$P(E) \propto e^{-E}.$$

Once the initial state of the particle is known, the particles travel through the detector. We use a first order Taylor expansion numerical integration to determine particle trajectories. The Lorentz force law is expanded in powers of spatial step size Δs (set to 100 μm), and the programs used magnetic field data for the Mu2e detector appropriate for each step.

When a particle is found inside the proton absorber, in each iteration step the particle loses energy. The energy loss each per step is given by the first order approximation

$$\Delta E = \frac{dE}{ds} \cdot \Delta s.$$

For electrons, the energy loss was based on bremsstrahlung and for protons the Bethe-Bloch equation was used for protons in polyethylene with a density of .94 gm/cm³. To account for the stochastic properties of energy loss, after the particles leave the absorber the actual energy loss is given by a distribution with mean value based on the previous calculation of energy loss in the absorber. For protons, a Gaussian distribution is used with a standard deviation in keV of

$$\sigma = 290.3 \cdot \sqrt{x}$$

where x is the distance traveled through the absorber in cm. For electrons, a Landau distribution is used with an RMS width based on the distance traveled through the absorber³.

Once electrons reach the tracker, 3.5 m

downstream of the target, the programs log the final position and momentum information of the particle and begin with a new particle. For protons, the programs continue until the particle passes beyond the tracker, 6 m downstream of the target. The programs also log whether the protons hit the tracker.

After the simulation programs finish, the stored final momentum information is used for statistical analysis. From this stored information, histograms of the final momenta and the final momenta assuming there was no fluctuation in energy loss can be plotted.

IV. Results and Discussion

From the data collected, information can be extracted about the percentage of protons that hit the tracker, electron final momentum, momentum resolution, and effects on a possible in situ calibration electron injected into the detector.

Monte Carlo simulations with 5000 particles show that, with a helical absorber, 2.8% of protons originating in the target hit the tracker. An analogous simulation shows that, with a cylindrical absorber, 14.0% of protons hit the tracker. So, this helical geometry reduces the background noise from protons by a factor of 5 in comparison to the conventional cylindrical design.

There are three classes of electrons that make it through the absorber region. There are those that lose over 5% of their energy and are no longer useful to the experiment, those that weave through the absorber, miss it, and lose no energy, and those that lose a small amount of energy, less than 5% of their initial energy.

We ran Monte Carlo simulations with 5000 particles and classified electrons according to their final momentum. The classification can be found in Table 1 for both absorbers. The results show that both absorbers will destroy about 10% of signal events. But, a very nice feature of the helical absorber is that over half of signal electrons manage to weave their way through the absorber without hitting any of the absorber. This will be advantageous when looking at resolution since it will give a class of signal electrons, representing about half of events, with no resolution smearing in the absorber.

Final e^- Momentum	105 MeV/c	< 99.75 MeV/c	$99.75 < p < 105$ MeV/c
Helical Absorber	52.8%	8.4%	38.8%
Cylindrical Absorber	0	13.0%	87.0%

Table 1. Percentage of electrons in each of the momentum classes described above.

In Figure 2 we plot the difference between the average energy loss $\Delta E_{classical}$ and the Landau-fluctuated energy loss $\Delta E_{statistical}$ for simulated electrons, defining $\xi \equiv \Delta E_{classical} - \Delta E_{statistical}$.

The standard deviation of this ξ distribution gives the resolution of the spectrometer with the given absorber. The histograms show the resolution for electrons which strike the helical absorber to be 267 keV, according to a simulation with 1000 particles. Note that signal electrons that avoid contact with the polyethylene absorber structure are *not* included in the histogram, so that a distribution which included these electrons has a smaller RMS width of 190 keV. We find that spectrometer resolution with a cylindrical absorber is 356 keV. This is in good agreement with the resolution of 351 keV for the same cylindrical absorber configuration described in Reference 2.

The data collected were also used to analyze the momentum loss of electrons for a possible in situ calibration of the detector. Since in this situation electrons are moving upstream, their trajectory resembles that of a proton traveling downstream, so calibration electrons will hit the detector as often as protons coming from the target. With these simulations, each testing 1000 particles, the resolution of calibration electrons traveling towards the target through a cylindrical absorber is 372 keV, which is in close agreement with the resolution of electrons originating in the target and traveling through a cylindrical absorber. The resolution in traveling through the helical absorber is 204 keV. So, adding these in quadrature with the results for particles traveling downstream, the total resolution of a cylindrical absorber is 515 keV when entering the tracker.

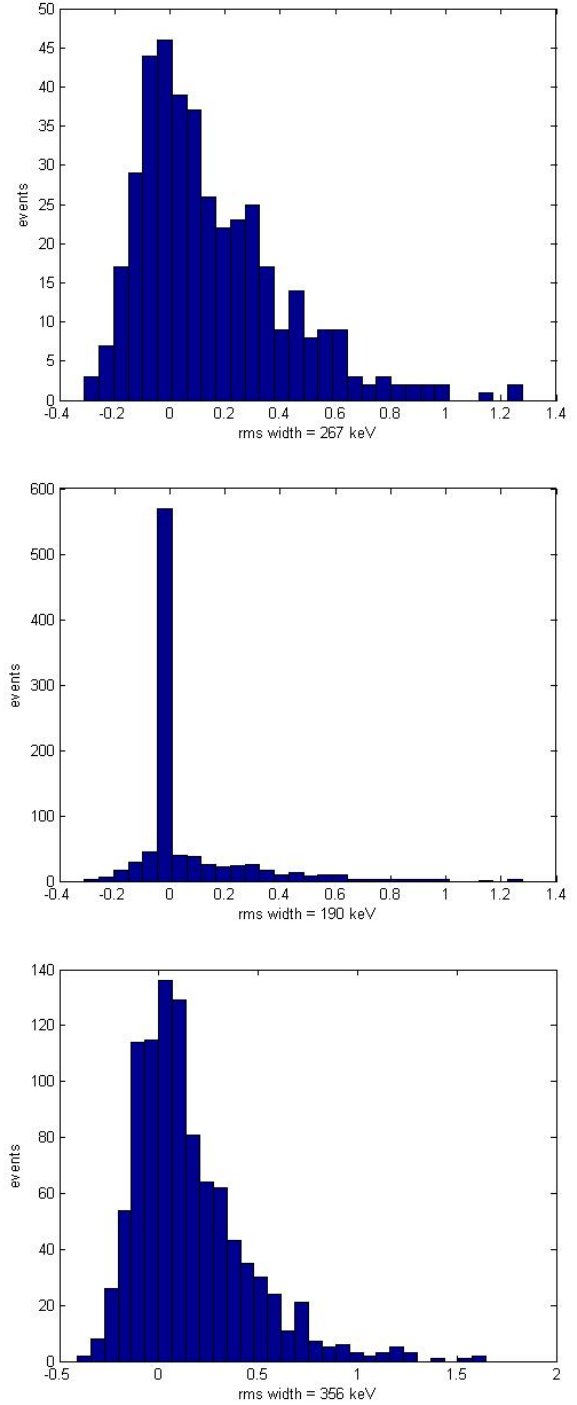


Figure 2. Top: ξ for a helical absorber including only particles striking the absorber. Middle: ξ for a helical absorber including all electrons passing through the absorber region. Bottom: ξ for a cylindrical absorber. Note the electrons that are untouched by the helical absorber are not included in the top histogram. ξ is defined in the text.

Calibration electrons traveling through a helical absorber will again be split into two categories of roughly equal size, one with a spread of 204 keV

and another with a spread of 336 keV when entering the tracker depending on whether the electron hits the absorber on the return track.

V. Conclusions

When comparing Monte Carlo simulation results for both the conventional cylindrical geometry and this novel helical shape, the data repeatedly show that a helical absorber outperforms a cylindrical absorber. A helix will substantially reduce the amount of proton background in the tracker and improve the momentum resolution of signal electrons. In addition, this absorber introduces a new class of electrons with no absorber straggling representing about half of the total events. The resolution of these particles is better than the resolution of signal electrons passing through a cylindrical absorber. There is little difference in resolution between the two absorbers when considering calibration electrons injected from the downstream end of the detector. This absorber, if installed in the Mu2e detector, would be a valuable asset to the experiment, collaboration, and the data collected.

VI. Acknowledgments

The author would like to thank Robert Coverdill for assistance with 3D printing to better visualize the geometry of this novel absorber design. Also, considerable appreciation goes to the National Science Foundation whose grant PHY-0647885, along with the University of Illinois Office of the Vice Chancellor for Research, funded this research project.

VII. References

- ¹Rob Kutschke. 2009. CIPANP Preceedings. Mu2e-doc-546-v6.
- ²Peter Kammel. 2009. Mu2e Test Run at PSI.
- ³A. B. Isaev and V. I. Popov. Izmeritel naya Tekhnika, No. 3. pp. 60-62. March, 1970.